J|A|C|S
ARTICLES

Published on Web 06/25/2009

Modeling the Multivalent Recognition between Dendritic Molecules and DNA: Understanding How Ligand "Sacrifice" and Screening Can Enhance Binding

Giovanni M. Pavan,*,†,‡ Andrea Danani,‡ Sabrina Pricl,†,‡ and David K. Smith*,§

Molecular Simulations Engineering (MOSE) Laboratory, Department of Chemical Engineering (DICAMP), University of Trieste, Piazzale Europa 1, 34127 Trieste, Italy, Institute of Computer Integrated Manufacturing for Sustainable Innovation (ICIMSI), University for Applied Sciences of Southern Switzerland (SUPSI), Centro Galleria 2, Manno, CH-6928, Switzerland, and Department of Chemistry, University of York, Heslington, York, YO10 5DD, U.K.

Received February 14, 2009; E-mail: giovanni.pavan@supsi.ch; dks3@york.ac.uk

Abstract: This paper reports the application of molecular dynamics methods to understand the interactions between dendritic molecules with spermine surface groups and double-helical DNA. Importantly, we are able to reproduce the binding effects observed experimentally, indicating that this type of modeling is robust and reliable. The energetic effects were deconvoluted in order to quantify the binding of each spermine unit to the DNA double helix. Importantly, for the first-generation dendron **G1**, DNA binding was adversely affected by increasing levels of NaCl (>10% of the interaction energy is lost). For second-generation **G2** however, we observed a compensation effect, in which some ligands "sacrifice" themselves, losing large amounts of binding energy with DNA. However, these ligands screen the complex, which enables the other spermine residues to bind more effectively to DNA. In this way, the multivalent array is able to maintain its high affinity binding, even as the salt concentration increases (only ca. 1% of the interaction energy is lost). These modeling studies are in agreement with, and provide a unique insight into, the experimental results. Clearly, ligand flexibility and ability to reorganize the interactions with DNA are important, demonstrating that high levels of preorganization and ligand framework rigidity are not always beneficial for multivalent recognition. The concept suggested by this modeling study, in which ligand "sacrifice" and binding site screening combine to enable high-affinity binding, is a new paradigm in multivalency.

Introduction

High-affinity molecular recognition of biomolecular targets is of crucial importance in the development of synthetic systems capable of intervening in biological pathways; multivalent recognition is a key principle in enhancing binding strength and hence developing systems with potential biomedical applications.[1] Experimental studies and mathematical models have demonstrated that once the first ligand in a multivalent array has bound to the target, the binding of a second ligand will be a cooperative, entropically less disfavored process, with a local concentration effect also enhancing binding.[2] There have been a number of studies in which multivalency has been directly modeled using computational methods; for example, the widely investigated interaction between oligosaccharides and lectins has been studied in some depth,[3] as have a range of other multivalent biological recognition processes.[4]

† University of Trieste.
‡ ICIMSI, SUPSI.
§ University of York.

(1) (a) Mammen, M.; Choi, S.-K; Whitesides, G. M. *Angew. Chem., Int. Ed.* **1998**, *37*, 2754–2794. (b) Mulder, A.; Huskens, J.; Reinhoudt, D. N. *Org. Biomol. Chem.* **2004**, *2*, 3409–3424. (c) Badjic, J. D.; Nelson, A.; Cantrill, S. J.; Turnbull, W. B.; Stoddart, J. F. *Acc. Chem. Res.* **2005**, *38*, 723–732.

(2) See for example: (a) Huskens, J.; Mulder, A.; Auletta, T.; Nijhuis, C. A.; Ludden, M. J. W.; Reinhoudt, D. N. *J. Am. Chem. Soc.* **2004**, *126*, 6784–6797. (b) Doyle, E. L.; Hunter, C. A.; Philips, H. C.; Webb, S. J.; Williams, N. H. *J. Am. Chem. Soc.* **2003**, *125*, 4593–4599. (c) Lim, C. W.; Ravoo, B. J.; Reinhoudt, D. N. *Chem. Commun.* **2005**, 5627–5629. (d) Mart, R. J.; Liem, K. P.; Wang, X.; Webb, S. J. *J. Am. Chem. Soc.* **2006**, *128*, 14462–14463. (e) Lim, C. W.; Crespo-Biel, O.; Stuart, M. C. A.; Reinhoudt, D. N.; Huskens, J.; Ravoo, B. J. *Proc. Natl. Acad. Sci. U.S.A.* **2007**, *104*, 6986–6991.

(3) (a) Marotte, K.; Eville, C. P.; Sabin, C.; Pymbock, M. M.; Imberty, A.; Roy, R. *Org. Biomol. Chem.* **2007**, *5*, 2953–2961. (b) Ramachandraiah, G.; Chandra, N. R.; Surolia, A.; Vijayan, M. *Glycobiology* **2003**, *13*, 765–775. (c) Natchiar, S. K.; Srinivas, O.; Mitra, N.; Dev, S.; Jayaraman, N.; Surolia, A.; Vijayan, M. *Curr. Sci.* **2006**, *90*, 1230–1237. (d) Gouin, S. G.; Vanquelef, E.; Fernandez, J. M. G.; Mellet, C. O.; Dupradeau, F. Y.; Kovensky, J. *J. Org. Chem.* **2007**, *72*, 9032–9045.

(4) See for example: (a) Lilja, A. E.; Jenssen, J. R.; Kahn, J. D. *J. Mol. Biol.* **2004**, *342*, 467–468. (b) Zhang, J. B.; Tanha, J.; Hirama, T.; Khieu, N. H.; To, R.; Hong, T. S.; Stone, E.; Brisson, J. R.; MacKenzie, C. R. *J. Mol. Biol.* **2004**, *335*, 49–56. (c) Handl, H. L.; Sankaranarayanan, R.; Josan, J. S.; Vagner, J.; Mash, E. A.; Gillies, R. J.; Hruby, V. J. *Bioconjugate Chem.* **2007**, *18*, 1101–1109. (d) Liu, Z.; Young, A. W.; Hu, P.; Rice, A. J.; Zhou, C.; Zhan, Y.; Kallenbach, N. R. *ChemBioChem* **2007**, *8*, 2063–2065. (e) Agrawal, N. J.; Radhakrishnan, R. *J. Phys. Chem. C* **2007**, *111*, 15848–15856. (f) Chang, T.; Pieterse, K.; Broeren, M. A. C.; Kooijman, H.; Spek, A. L.; Hilbers, P. A. I.; Meijer, E. W. *Chem.—Eur. J.* **2007**, *13*, 7883–7889.

(5) (a) Newkome, G. R.; Moorefield, C. N.; Vögtle, F. *Dendrimers and Dendrons: Concepts, Syntheses, Applications*; VCH: Weinheim, 2001. (b) Fréchet, J. M. J.; Tomalia, D. A. *Dendrimers and Other Dendritic Polymers*; John Wiley and Sons: New York, 2002. (c) Smith, D. K. *Tetrahedron* **2003**, *59*, 3797–3798. (d) Tomalia, D. A. *Prog. Polym. Sci.* **2005**, *30*, 294–324.

 10.1021/ja901174k CCC: $40.75

One of the most effective ways of organizing a multivalent array of ligating groups is to use a dendritic scaffold. Dendrimers and dendrons are well-defined branched polymers that have repetitive structures.[5] When the multiple surface groups are ligands, the dendritic scaffolding can be considered to act as a kind of nanoscaffolding, organizing the ligand array. As such, dendritic systems have been widely exploited for their potential applications in multivalent biological recognition.[6] Much of the early work focused on arrays of oligosaccharides and quantified the advantages that could be gained by the dendritic arrangement of such ligands.[7] There has also been considerable interest in the ability of dendritic structures to act in a multivalent way to prevent viral uptake, with particular focus on herpes and HIV as targets for intervention.[8] Modeling studies have highlighted the influence of shape on anti-HIV efficiency. DNA-binding dendrimers have been an area of considerable interest,[9] an area of work pioneered by the groups of Tomalia and Szoka, who used poly(amidoamine) (PAMAM) dendrimers.[10] These polycationic, multivalent dendrimers show high affinity for DNA and can achieve gene delivery into cells.[11] Computer modeling of the interactions between these dendrimers and single-strand DNA suggested that at high dendritic generations of growth DNA wrapped itself around the large surface of the dendrimer, a process that is conceptually related to the interaction between DNA and polycationic chromatin in the cell nucleus.[12] Since these studies, a wide range of polycationic multivalent dendrimers and dendrons have been employed in DNA binding and gene delivery, including systems based on dendritic poly(L-lysine),[13] poly(propyleneimine),[14] and other more specialized dendritic frameworks.[15] In general, the affinity for DNA increases with dendritic generation; that is, as the dendritic molecules become larger, and more highly charged, binding of polyanionic DNA is enhanced. The gene delivery profiles also improve at higher dendritic generation; it is often argued that this is a consequence of the ability of excess amine groups to buffer pH within the endosome and hence mediate endosomal escape.[16]

We have recently developed a biomimetic approach to multivalent dendritic systems, reporting dendritic arrays of spermine (Figure 1) and demonstrating their ultrahigh affinities for DNA binding.[17] Spermine is a naturally occurring tetraamine that is used in nature for DNA binding.[18] It is an essential cellular component, being present at millimolar levels.[19] Spermine is also widely used to assist in the crystallization of DNA, and it is well-known that spermine (and related oligoamines such as spermidine) can induce DNA compaction, bundling, and aggregation.[20] The binding between oligoamines and DNA has been quite extensively investigated and computationally modeled using a range of different methodologies.[21] In particular, there has been considerable interest in the interplay between the DNA binding of tri- and tetracationic amines (spermidine/spermine) and monocations such as sodium.[22] It is largely accepted that monovalent cations are present in close vicinity to electronegative sites of the bases in the grooves and

(6) (a) Boas, U.; Christensen, J. B.; Heegaard, P. M. H. *Dendrimers in Medicine and Biotechnology*; RSC: Cambridge, 2006. (b) Stiriba, S. E.; Frey, H.; Haag, R. *Angew. Chem., Int. Ed.* **2002**, *41*, 1329–1334. (c) Svenson, S.; Tomalia, D. A. *Adv. Drug Delivery Rev.* **2005**, *57*, 2106–2129. (d) Villalonga-Barber, C.; Micha-Screttas, M.; Steele, B. R.; Georgopoulos, A.; Demetzos, C. *Curr. Top. Med. Chem.* **2008**, *8*, 1294–1309.

(7) Chabre, Y. M.; Roy, R. *Curr. Top. Med. Chem.* **2008**, *8*, 1237–1285.

(8) (a) Jiang, Y. H.; Emau, P.; Cairns, J. S.; Flanary, L.; Morton, W. R.; McCarthy, T. D.; Tsai, C. C. *Aids Res. Hum. Retroviruses* **2005**, *21*, 207–213. (b) Gong, E.; Matthews, B.; McCarthy, T.; Chu, J. H.; Holan, G.; Raff, J.; Sacks, S. *Antiviral Res.* **2005**, *68*, 139–146. (c) Patton, D. L.; Sweeeney, Y. T. C.; McCarthy, T. D.; Hillier, S. L. *Antimicrob. Agents Chemother.* **2006**, *50*, 1696–1700. (d) McCarthy, T. D.; Karellas, P.; Henderson, S. A.; Giannis, M.; O'Keefe, D. F.; Heery, G.; Paull, J. R. A.; Matthews, B. R.; Holan, G. *Mol. Pharm.* **2005**, *2*, 312–318. (e) Blanzat, M.; Turrin, C. O.; Aubertin, A. M.; Couturier-Vidal, C.; Caminade, A.-M.; Majoral, J.-P.; Rico-Lattes, I.; Lattes, A. *ChemBioChem* **2005**, *6*, 2207–2213.

(9) (a) Dufes, C.; Uchegbu, I. F.; Schatzlein, A. G. *Adv. Drug Delivery Rev.* **2005**, *57*, 2177–2202. (b) Guillot-Nieckowski, M.; Eisler, S.; Diederich, F. *New J. Chem.* **2007**, *31*, 1111–1127. (c) Parekh, H. S. *Curr. Pharm. Des.* **2007**, *13*, 2837–2850. (d) Smith, D. K. *Curr. Top. Med. Chem.* **2008**, *8*, 1187–1203. (e) Caminade, A.-M.; Turrin, C. O.; Majoral, J.-P. *Chem.—Eur. J.* **2008**, *14*, 7422–7432.

(10) (a) Haensler, J.; Szoka, F. C. *Bioconjugate Chem.* **1993**, *4*, 372–379. (b) Kukowska-Latallo, J. F.; Bielinska, A. U.; Johnson, J.; Spindler, R.; Tomalia, D. A.; Baker, J. R. *Proc. Natl. Acad. Sci. U.S.A.* **1996**, *93*, 4897–4902. (c) Bielinska, A.; Kukowska-Latallo, J. F.; Johnson, J.; Tomalia, D. A.; Baker, J. R. *Nucleic Acids Res.* **1996**, *24*, 2176–2182. (d) Tang, M. X.; Redemann, C. T.; Szoka, F. C. *Bioconjugate Chem.* **1996**, *7*, 703–714.

(11) Selected references include: (a) Tang, M. X.; Szoka, F. C. *Gene Ther.* **1997**, *4*, 823–832. (b) Bielinska, A. U.; Chen, C. L.; Johnson, J.; Baker, J. R. *Bioconjugate Chem.* **1999**, *10*, 843–850. (c) Malik, N.; Wiwattanapatapee, R.; Klopsch, R.; Lorenz, K.; Frey, H.; Weener, J. W.; Meijer, E. W.; Paulus, W.; Duncan, R. *J. Controlled Release* **2000**, *65*, 133–148. (d) Luo, D.; Haverstick, K.; Belcheva, N.; Han, E.; Saltzman, W. M. *Macromolecules* **2002**, *35*, 3456–3462. (e) Abdelhady, H. G.; Allen, S.; Davies, M. C.; Roberts, C. J.; Tendler, S. J. B.; Williams, P. M. *Nucleic Acids Res.* **2003**, *31*, 4001–4005. (f) Zhou, J.; Wu, J.; Hafdi, N.; Behr, J.-P.; Erbacher, P.; Peng, L. *Chem. Commun.* **2006**, 2362–2364. (g) Takahashi, T.; Kojima, C.; Harada, A.; Kono, K. *Bioconjugate Chem.* **2007**, *18*, 1349–1354.

(12) (a) Chen, W.; Turro, N. J.; Tomalia, D. A. *Langmuir* **2000**, *16*, 15–19. (b) Lyulin, S. V.; Darinskii, A. A.; Lyulin, A. V. *Macromolecules* **2005**, *38*, 3990–3998. (c) Maiti, P. K.; Bagchi, B. *Nano Lett.* **2006**, *6*, 2478–2485.

(13) Selected references include: (a) Ohsaki, M.; Okuda, T.; Wada, A.; Hirayama, T.; Niidome, T.; Aoyagi, H *Bioconjugate Chem* **2002**, *13*, 510–517. (b) Toth, I.; Sakthivel, T.; Wilderspin, A. F.; Bayele, H.; O'Donnell, M.; Perry, D. J.; Pasi, K. J.; Lee, C. A.; Florence, A. T. *STP Pharm. Sci.* **1999**, *9*, 93–99. (c) Choi, J. S.; Joo, D. K.; Kim, C. H.; Kim, K.; Park, J.-S. *J. Am. Chem. Soc.* **2000**, *122*, 474–480. (d) Kiselev, A. V.; Il'ina, P. L.; Egorova, A. A.; Baranov, A. N.; Guryanov, I. A.; Bayanova, N. V.; Tarasenko, I. I.; Lesina, E. A.; Vlasov, G. P.; Baranov, V. S. *Russ. J. Gen.* **2007**, *43*, 593–600.

(14) See for example: (a) Zinselmeyer, B. H.; Mackay, S. P.; Schatzlein, A. G.; Uchegbu, I. F. *Pharm. Res.* **2002**, *19*, 960–967. (b) Kim, T.-i.; Baek, J.-u.; Bai, C. Z.; Park, J.-S. *Biomaterials* **2007**, *28*, 2061–2067.

(15) (a) Joester, D.; Losson, M.; Pugin, R.; Heinzelmann, H.; Walter, E.; Merkle, H. P.; Diederich, F. *Angew. Chem., Int. Ed.* **2003**, *42*, 1486–1490. (b) Loup, C.; Zanta, M.-A.; Caminade, A.-M.; Majoral, J.-P.; Meunier, B. *Chem.—Eur. J.* **1999**, *5*, 3644–3650. (c) Maksimenko, A. V.; Mandrouguine, V.; Gottikh, M. B.; Bertrand, J.-R.; Majoral, J.-P.; Malvy, C. *J. Gene Med.* **2005**, *5*, 61–71. (d) Guillot, M.; Eisler, S.; Weller, K.; Merkle, H. P.; Gallani, J.-L.; Diederich, F. *Org. Biomol. Chem.* **2006**, *4*, 766–769.

(16) Sonawane, N. D.; Szoka, F. C.; Verkman, A. S. *J. Biol. Chem.* **2003**, *278*, 44826–44831.

(17) Kostiainen, M. A.; Hardy, J. G.; Smith, D. K. *Angew. Chem., Int. Ed.* **2005**, *44*, 2556–2559.

(18) (a) Tabor, C. W.; Tabor, H. *Annu. Rev. Biochem.* **1984**, 740–790. (b) Vijayanathan, V.; Thomas, T.; Shirahata, A.; Thomas, T. J. *Biochemistry* **2001**, *40*, 13644–13651. (c) Igarashi, K.; Kashiwagi, K. *Biochem. Biophys. Res. Commun.* **2000**, *271*, 559–564. (d) Patel, M. M.; Anchordoquy, T. J. *Biophys. Chem.* **2006**, *122*, 5–15.

(19) (a) Cohen, S. S. *A Guide to Polyamines*; Oxford University Press: Oxford, 1998. (b) Igarashi, K.; Kashiwagi, K. *Biochem. Biophys. Res. Commun.* **2000**, *271*, 559–564.

(20) (a) Gosule, L. C.; Schellman, J. A. *Nature* **1976**, *259*, 333–335. (b) Wilson, R. W.; Bloomfield, V. A. *Biochemistry* **1979**, *79*, 2192–2196. (c) Timsit, Y.; Moras, D. *Methods Enzymol.* **1992**, *211*, 409–429. (d) Korolev, N.; Lyubartsev, A. P.; Nordenskiöld, L.; Laaksonen, A. *J. Mol. Biol.* **2001**, *308*, 907–917. (e) Sines, C. C.; McFail-Isom, L.; van Derveer, L.; Williams, L. D. *J. Am. Chem. Soc.* **2000**, *122*, 11048–11056. (f) Raspaud, E.; Olivera de la Cruz, M.; Sikorav, J.-L.; Livolant, F. *Biophys. J.* **1998**, *74*, 381–393. (g) Deng, H.; Bloomfield, V. A.; Benevides, J. M.; Thomas, G. R. Jr. *Nucleic Acids Res.* **2000**, *28*, 3379–3385. (h) Tippin, D. B.; Sundaralingam, M. *J. Mol. Biol.* **1997**, *267*, 1171–1185.

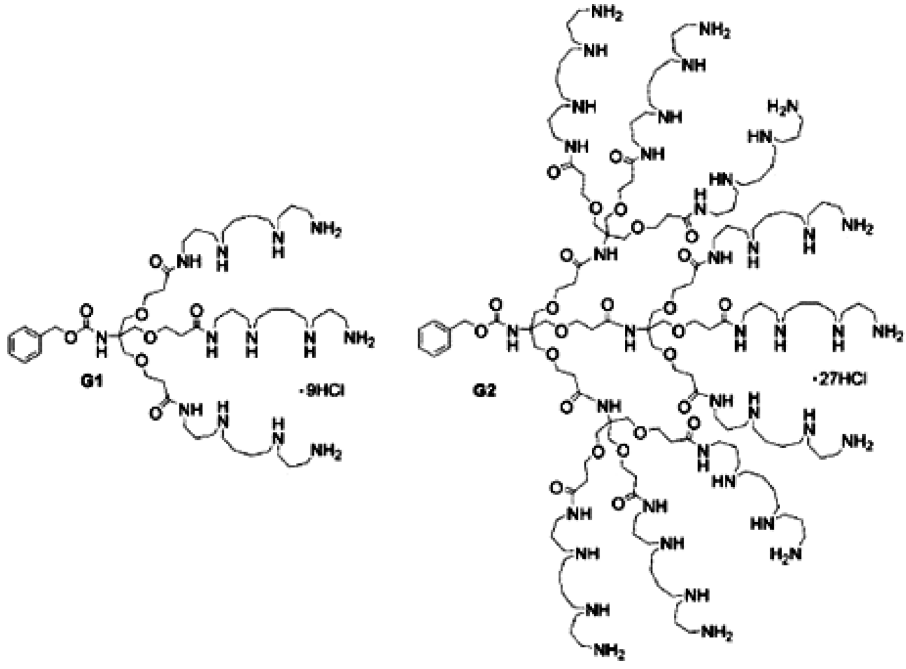

Figure 1. Chemical structures of dendrons modeled in this paper.

the anionic phosphate groups and that a cationic ligand such as spermine has to compete with these cations to achieve binding. The relatively high biological concentrations of Na^+ (>100 mM) mean that relatively large quantities of spermine are required to effectively bind DNA.

Our multivalent array of spermine ligands on a dendritic support (Figure 1) gave rise to high-affinity DNA binding, even at low concentrations.[17] We employed an ethidium bromide (EthBr) displacement assay to gain a comparative quantitative estimate of the binding strengths and discovered that the second-generation system (**G2**), with nine surface spermine ligands, displaced 50% of EthBr from its complex with DNA at concentrations as low as 30 nM. This was a significantly lower concentration than the high micromolar levels required for monovalent spermine. Furthermore, we found that the binding of **G2** to DNA, unlike monovalent or trivalent spermine arrays (**G1**), was remarkably independent of sodium chloride concentration. Since this preliminary study, we have grafted this dendritic spermine array onto proteins and demonstrated that the synthetic nanoscale biohybrids exhibit high DNA affinity.[23] We have also modified the structures of the dendrons such that cellular gene delivery can be achieved.[24] Finally, we have developed degradable multivalent systems, in which the spermine ligands are cleaved from the surface of the dendron, effectively "switching off" the high-affinity binding.[25] However, we remained fundamentally interested in how the array of spermine ligands gave rise to the two multivalent binding effects: (i) high affinity and (ii) NaCl-independent binding. As such, we decided to apply a molecular dynamics modeling approach to shed further light on the mode of binding. The results are presented in this paper. We can rationalize the binding strengths observed for the dendrons and, importantly, generate a new understanding of multivalency effects in which some ligands sacrifice their binding in order to partially screen the interaction site from competitor species, hence helping protect the recognition event.

Computational Details

All simulations and data analysis were performed with the AMBER 9 suite of programs.[26] A 21 base-pair double-stranded B-DNA was generated with the *nucgen* module of AMBER 9. Each dendron structure was built using three different residue types: a central (CEN), a repetitive (REP), and a terminal, charged (+3) spermine unit (SPM). The force field parameters for these residue

(21) (a) Feuerstein, B. G.; Pattabiraman, N.; Marton, L. J. *Nucleic Acids Res.* **1989**, *17*, 6883–3892. (b) Feuerstein, B. G.; Pattabiraman, N.; Marton, L. J. *Nucleic Acids Res.* **1990**, *18*, 1271–1282. (c) Haworth, I. S.; Rodger, A.; Richards, W. G. *Proc. R. Soc. B* **1991**, *244*, 107–116. (d) Lyubartsev, A. P.; Nordenskiöld, L. *J. Phys. Chem. B* **1997**, *101*, 4335–4342. (e) Rouzina, I.; Bloomfield, V. A. *Biophys. J.* **1998**, *74*, 3152–3164. (f) Dias, R. S.; Pais, A. A. C. C.; Miguel, M. G.; Lindman, B. *J. Chem. Phys.* **2003**, *119*, 8150–8157. (g) Real, A. N.; Greenall, R. J. *J. Biomol. Struct. Dynam.* **2003**, *21*, 469–487. (h) Deserno, M.; Arnold, A.; Holm, C. *Macromolecules* **2003**, *36*, 249–259. (i) Teif, V. B *Biophys. J.* **2005**, *89*, 2574–2587. (j) Saito, T.; Iwaki, T.; Yoshikawa, K. *Europhys. Lett.* **2005**, *71*, 304–310. (k) Pastre, D.; Pietrement, O.; Landousy, F.; Hamon, L.; Sorel, I.; David, M. O.; Delain, E.; Zozime, A.; Le Cam, E. *Eur. Biophys. J. Biophys. Lett.* **2006**, *35*, 214–223. (l) Sanchez-Causasco, S.; Delcros, J. G.; Moya-Garcia, A. A.; Sanchez-Jimenez, F.; Ramirez, F. J. *Biophys. Chem.* **2008**, *133*, 54–65. (m) Dai, L.; Mu, Y. G.; Nordenskiöld, L.; van der Maarel, J. R. C. *Phys. Rev. Lett.* **2008**, *100*, 118301.

(22) (a) Korolev, N.; Lyubartsev, A. P.; Laaksonen, A.; Nordenskiöld, L. *Biophys. J.* **2002**, *82*, 2860–2875. (b) Korolev, N.; Lyubartsev, A. P.; Laaksonen, A.; Nordenskiöld, L. *Nucleic Acids Res.* **2003**, *30*, 5971–5981. (c) Korolev, N.; Lyubartsev, A. P.; Laaksonen, A.; Nordenskiöld, L. *Eur. Biophys. J.* **2004**, *33*, 671–682. (d) Burak, Y.; Ariel, G.; Andelman, D. *Curr. Opin. Colloid, Interface Sci.* **2004**, *9*, 53–58. (e) Allahyarov, E.; Löwen, H.; Gompper, G. *Phys. Rev. E* **2003**, *68*, 061903.

(23) (a) Kostiainen, M. A.; Szilvay, G. R.; Smith, D. K.; Linder, M. B.; Ikkala, O. *Angew. Chem., Int. Ed.* **2006**, *45*, 3538–3542. (b) Kostiainen, M. A.; Szilvay, G. R.; Lehtinen, J.; Smith, D. K.; Linder, M. B.; Urtti, A.; Ikkala, O. *ACS Nano* **2007**, *1*, 103–113.

(24) (a) Hardy, J. G.; Kostiainen, M. A.; Smith, D. K.; Gabrielson, N. P.; Pack, D. W. *Bioconjugate Chem.* **2006**, *17*, 172–178. (b) Jones, S. P.; Gabrielson, N. P.; Pack, D. W.; Smith, D. K. *Chem. Commun.* **2008**, 4700–4702.

(25) (a) Kostiainen, M. A.; Smith, D. K.; Ikkala, O. *Angew. Chem., Int. Ed.* **2007**, *46*, 7600–7604. (b) Welsh, D. J.; Jones, S. P.; Smith, D. K. *Angew. Chem., Int. Ed.* **2009**, *48*, 4047–4051.

(26) Case, D. A.; Darden, T. A.; Cheatham, T. E.; et al. *AMBER 9*; University of California: San Francisco, CA, 2006.

Table 1. Main Features of the Dendron/DNA Complexes Simulated in This Work

complex	[NaCl] (mM)	water box volume (Å^3)	dendron charge[b]	total number of added NaCl molecules	total number of counterion atoms[a]
G1	150	321 840	+9	29	89
3×G1	150	548 898	+27	50	113
G2	150	470 895	+27	43	99
G1	9.4	321 840	+9	2	35
3×G1	9.4	548 898	+27	3	19
G2	9.4	470 895	+27	3	19

[a] The total number of counterions in the last column is the sum of the counterions required for system neutralization and the Na^+ and Cl^- ions added to reproduce the experimental ionic concentration (2nd column). [b] The 21 base-pair DNA charge has an overall charge of −40; the terminal nucleotides do not carry a charge in the model.

types were obtained using the *antechamber* module of AMBER 9. Each dendron generation (**G1** and **G2**) was then solvated in a TIP3P water box,[27] extending 12 Å from the solute in the three dimensions. A suitable number of counterions were added to neutralize the system using the *leap* module of AMBER 9, removing eventual overlapping water molecules. The resulting systems, containing the dendrons, ions, and water, were first minimized and then equilibrated by running 10 ns NPT molecular dynamics simulations.

From the corresponding equilibrated systems, the water molecules and counterions were removed, and the B-DNA molecule was placed with its major groove in the proximity of the **G1** and **G2** dendrons, respectively. Thus, two 1:1 systems (**G1**+DNA and **G2**+DNA) were generated. Another system, composed of three **G1** and one DNA molecules (**3×G1**), was created in order to compare the effect of three **G1** molecules (total charge +27) (3**G1**+DNA) and one single **G2** molecule (total charge +27) on the DNA-binding energetics. All resulting structures were again solvated with a water box extending 12 Å from the solute in the case of the **G1** system and 14 Å in the case of the **3×G1** and **G2** systems, respectively. Counterions were then added in two steps: first, only the counterions necessary to ensure system neutrality were introduced, while, in a further step, the proper amount of Na^+ and Cl^- ions was added to reproduce the correct experimental salt concentration. Overall, six molecular systems were prepared: **G1** and **G2** dendrons in 1:1 complex with DNA (both at ionic strength of 9.4 and 150 mM NaCl, respectively) and two further systems composed of **G1** dendron complexed with DNA in a 3 to 1 ratio (**3×G1**) (at 9.4 and 150 mM NaCl). Table 1 summarizes the main characteristics of the simulated systems.

Each system was energy minimized and then equilibrated at 300 K by 50 ps molecular dynamics under NVT conditions. This stage was followed by a density equilibration run (50 ps) under NPT conditions. The production phase lasted 10 ns under periodic boundary condition at 300 K and 1 atm, using a time step of 2 fs, the Langevin thermostat, and a 10 Å cutoff. The particle mesh Ewald[28] (PME) approach was adopted to treat long-range electrostatic effects, and bond lengths involving bonds to hydrogen atoms were constrained using the SHAKE algorithm.[29]

All of the production molecular dynamics (MD) simulations were carried out by using the *sander* and *pmemd* module within the AMBER 9 suite of programs and the *parm99* all-atom force field by Cornell et al.[30] working in parallel on 32 processors of the IBM/BCX calculation cluster of the CINECA calculation center of Bologna. Table 2 summarizes simulation conditions.

Table 2. Simulation Conditions[a]

complex	[NaCl] (mM)	cutoff radius (Å)	simulation time (ns)	number of water molecules in the system	total number of atoms in the system
G1	150	10	10	7847	25 149
3×G1	150	10	10	14 094	44 501
G2	150	10	10	11 885	37 843
G1	9.4	10	10	7901	25 311
3×G1	9.4	10	10	14 188	44 783
G2	9.4	10	10	11 965	38 083

[a] For 10 ns of simulations run in parallel on 32 Opteron Dual Core 2.6 GHz processors on the IBM BCX/5120 cluster of the CINECA supercomputer center in Bologna, Italy.

All energetic analyses were performed for a single 10 ns MD trajectory of each dendron/DNA complex considered, with 200 unbound dendron and substrate snapshots taken from the frames in the equilibrated data production phase of that trajectory. The binding free energy for each ligand/receptor system, ΔG_{bind}, was calculated according to the molecular mechanics/Poisson−Boltzmann surface area method (MM-PBSA)[31] as

$$\Delta G_{bind} = \Delta H_{bind} - T\Delta S_{bind} \quad (1)$$

$$\Delta H_{bind} = E_{gas} + \Delta G_{sol} \quad (2)$$

The average values of the enthalpic contribution to ΔG_{bind} were calculated by summing the gas-phase energies ($E_{gas} = E_{ele} + E_{vdw}$) and the solvation free energies ($\Delta G_{sol} = \Delta G_{PB} + \Delta G_{NP}$).[32]

The polar component of ΔG_{sol} was evaluated using the Poisson−Boltzmann (PB) approach,[33] while the nonpolar contribution to the solvation energy was calculated as $\Delta G_{NP} = \gamma(\text{SASA}) + \beta$, in which $\gamma = 0.00542$ kcal/Å^2, $\beta = 0.92$ kcal/mol, and SASA is the solvent-accessible surface estimated with the MSMS program.[34] Finally, the normal-mode analysis approach was applied to 100 MD frames to estimate the last parameter, i.e., the entropic contributions ($-T\Delta S_{bind}$).[35]

In order to examine the individual contribution of the dendron residues to DNA binding, the collected MD frames of the 1:1 complexes (both for **G1** and **G2** at both ionic strengths) were further processed with the *mm_pbsa.pl* script of AMBER 9. Accordingly, the interaction energy between each CEN, REP, and SPM dendron residue and DNA was calculated, decomposing the affinity energy on a per residue basis in terms of gas-phase and desolvation contributions, utilizing the generalized Born method.[36]

Results and Discussion

Experimentally, the binding of dendrons **G1** and **G2** to DNA had previously been assessed using an ethidium bromide (EthBr) exclusion assay.[17,37] For clarity, these data are briefly described here. In this experiment, EthBr was first bound to calf thymus DNA, and then the concentration of dendron required to reduce the fluorescence intensity of EthBr

(27) Jorgensen, W. L.; Chandrasekhar, J.; Madura, J. D.; Impey, R. W.; Klein, M. L. *J. Chem. Phys.* **1983**, *79*, 926–35.
(28) Darden, T.; York, D.; Pedersen, L. *J. Chem. Phys.* **1998**, *98*, 10089–10092.
(29) (a) Ryckaert, J.-P.; Ciccotti, G.; Berendsen, H. J. C. *J. Comput. Phys.* **1977**, *23*, 327. (b) Krautler, V.; van Gunsteren, W. F.; Hanenberger, P. H. *J. Comput. Chem.* **2001**, *5*, 501.
(30) Cornell, W. D.; Cieplak, P.; Bayly, C. I.; Gould, I. R.; Merz, K. M.; Ferguson, D. M.; Spellmeyer, D. C.; Fox, T.; Caldwell, J. W.; Kollman, P. A. *J. Am. Chem. Soc.* **1995**, *117*, 5179–5197.
(31) Srinivasan, J.; Cheatham, T. E.; Cieplak, P.; Kollman, P. A.; Case, D. A. *J. Am. Chem. Soc.* **1998**, *120*, 9401–09.
(32) Jayaram, B.; Sprous, D.; Beveridge, D. L. *J. Phys. Chem.* **1998**, *102*, 9571–9576.
(33) Sitkoff, D.; Sharp, K. A.; Honig, B. *J. Phys. Chem.* **1994**, *98*, 1978–1988.
(34) Sanner, M. F.; Olson, A. J.; Spehner, J. C. *Biopolymers* **1996**, *38*, 305–20.
(35) Andricioaei, I.; Karplus, M. *J. Chem. Phys.* **2001**, *115*, 6289–92.
(36) Kollman, P. A.; Massova, I.; Reyes, C.; Kuhn, B.; Huo, S.; Chong, L.; Lee, M.; Lee, T.; Duan, Y.; Wang, W.; Donini, O.; Cieplak, P.; Srinivasan, J.; Case, D. A.; Cheatham, T. E. *Acc. Chem. Res.* **2000**, *33*, 889–897.
(37) (a) Cain, B. F.; Baguley, B. C.; Denny, W. A. *J. Med. Chem.* **1978**, *21*, 658–668. (b) Gershon, H.; Ghirlando, R.; Guttman, S. B.; Minsky, A. *Biochemistry* **1993**, *32*, 7143–7151. (c) Delcros, J. G.; Sturkenboom, M. C. J. M.; Basu, H. S.; Shafer, R. H.; Azollosi, J.; Feuerstein, B. J.; Marton, L. J. *Biochem. J.* **1993**, *291*, 269–274.

Table 3. Previously Reported Experimental Data for the Binding of **G1** and **G2** to Calf Thymus DNA as Determined by EthBr Displacement Assay[17a]

dendron	C_{50}[b] (nM) 9.4 mM NaCl	C_{50}[b] (nM) 150 mM NaCl	CE_{50}[c] 9.4 mM NaCl	CE_{50}[c] 150 mM NaCl
G1	76	300	0.61	2.70
G2	30	28	0.81	0.76

[a] Higher C_{50} and CE_{50} values represent less effective binding of the dendron to DNA. [b] C_{50} represents the concentration (in nM) of dendron required to displace 50% of the EthBr ([DNA base] = 1 μM, [EthBr] = 1.26 μM). [c] CE_{50} represents the charge excess (ratio of protonatable nitrogen atoms on the dendron to deprotonatable phosphate groups on the DNA) at which 50% of EthBr is displaced.

by 50% through competitive binding was determined. These concentrations (C_{50} values) are presented in Table 3 and represent the effective binding of the dendron to DNA. The lower the value, the more effective the binding, as a smaller molar amount of dendron is required. The data are also presented as charge excess (CE_{50}) values, where CE_{50} represents the charge excess of cationic dendron to anionic DNA required to reduce the EthBr fluorescence intensity by 50%. These CE_{50} values are effectively normalized *per amine* in the dendron and, therefore, reflect the multivalency of the dendron−DNA interaction.

The data demonstrated that under low salt conditions, **G2** bound to DNA at a lower concentration than **G1**. Indeed, achieving DNA binding using this type of assay at concentrations as low as 30 nM is remarkably high-affinity binding.[38] However, comparing CE_{50} values clearly demonstrates that under low salt conditions the effective amount of amine required to bind DNA was actually optimized for **G1**, probably indicating that not all of the amines of **G2** are directly involved in, or required for, DNA binding. Under high salt conditions, **G2** could still bind DNA at low nanomolar concentrations, whereas for **G1** the concentration of dendron required increased significantly. Indeed, under these conditions, the CE_{50} value indicated that per amine, **G2** was far more effective as a DNA binder than **G1**, an example of multivalency in action.

In order to model the interaction between the dendrons and DNA, we used a 21-base-pair B-DNA double strand containing a mixture of bases (Figure 2). This choice relied on a compromise between accuracy and computational feasibility. Both **G1** and **G2** dendron structures are quite small when compared to DNA, and a 21 base-pair long DNA therefore represents the ideal balance to ensure a correct binding mode but limit the water box dimensions, thus keeping CPU times to reasonable limits. For the purposes of modeling, we assumed that **G1** had nine protonated amines, while **G2** had 27 protonated amines. Both **G1** and **G2** were simulated in a water box, with a single DNA double helix and a single dendron unit (e.g., Figure 3), and binding affinities (ΔG_{bind}) were determined using molecular dynamics methods under both low (9.4 mM) and high (150 mM) salt conditions (see Computational Details section for further information). This mimics the previously reported experimental studies, which were performed under these conditions (Table 3). The computational energies are reported as an average across a number of snapshots obtained from the molecular dynamics trajectories.

According to the MM/PBSA simulation scheme, the binding energies ΔG_{bind} (Table 4) can be divided into enthalpic and entropic terms, ΔH_{bind} and ΔS_{bind} (eq 1). The enthalpic term, ΔH_{bind}, can be further split into the sum of noncovalent interactions between receptor and ligand in vacuum (E_{gas}) and a solvation correction (ΔG_{sol}) according to eq 2. The more negative the value of ΔG_{bind}, the greater the affinity between dendron and DNA. By comparing the data modeled under low and high salt conditions in terms of differences in thermodynamic parameters, we were able to evaluate the dependence on salt concentration. On analyzing the data in Table 4, it is immediately apparent that the calculations based on dendron **G1** (considering the presence of either one or three dendrons) exhibit pronounced salt dependency, i.e., nonzero and non-negligible difference in ΔG_{bind} values. On the other hand, it is immediately apparent that the overall binding affinity of **G2** to DNA does not appear to depend in any significant way on the concentration of NaCl. Furthermore, the decrease in ΔG_{bind} values for **G1** of 1.3 kcal mol^{-1} would reflect a weakening in

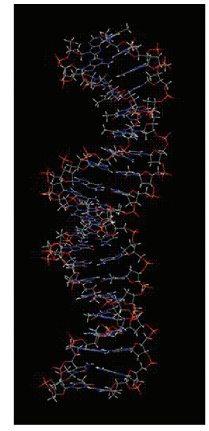

Anti-Sense: 5'-TCG AAG TAC TCA GAG TAA GTT-3'
Sense: 3'-AGC TTC ATG AGT CTC ATT CAA-5'

Figure 2. Structure of the double-helical DNA used for modeling in this paper.

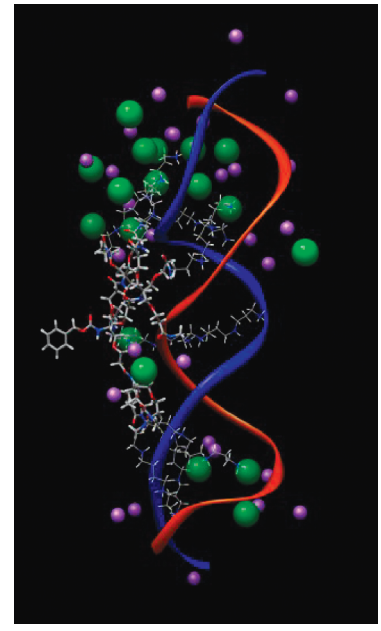

Figure 3. Model of **G2** dendron bound to DNA at 150 mM NaCl concentration. DNA double helix shown in ribbon form, dendron **G2** shown as atomic structure, Na^+ (purple), Cl^- (green).

(38) Zadmard, R.; Schrader, T. *Angew. Chem., Int. Ed.* **2006**, *45*, 2703–2706.

Table 4. Thermodynamic Parameters Determined by Molecular Dynamics Methods for the Binding of Dendrons **G1** and **G2** to DNA[a]

	9.4 mM NaCl			150 mM NaCl		
dendron	ΔH_{bind}	$-T\Delta S_{bind}$	ΔG_{bind}	ΔH_{bind}	$-T\Delta S_{bind}$	ΔG_{bind}
G1	−114.8 ± 11.3	+53.1 ± 10.4	−61.7	−106.3 ± 12.3	+45.9 ± 17.0	−60.4
G2	−310.0 ± 16.1	+113.9 ± 13.7	−196.2	−310.2 ± 11.5	+114.0 ± 14.4	−196.2
3×G1	−311.9 ± 10.2	+92.1 ± 19.9	−219.8	−316.9 ± 16.3	+99.7 ± 15.2	−217.3

[a] Analysis performed at two different salt concentrations. All data are in kcal mol^{-1}.

binding by approximately an order of magnitude, a significant change. Clearly, in general terms, these molecular dynamics calculations appear to be in agreement with the experimental data presented in Table 3.

For each system, the enthalpy of binding is negative (favorable), as is the entropy (unfavorable). This indicates that recognition between the dendron surface and the DNA double helix is, as might have been expected, enthalpically driven by the electrostatic interactions between the protonated amines and the anionic phosphate groups. The entropy decreases because the complex is more ordered than the individual components. It is interesting to note that the enthalpy of interaction (ΔH_{bind}) between **G1** and DNA is significantly affected by the increase in salt concentration (decrease in magnitude of 8.5 kcal mol^{-1}). On the other hand, the enthalpy of interaction between **G2** and DNA is effectively and surprisingly unaffected by the increase in salt concentration. Similarly, the entropy of binding between **G1** and DNA is perturbed (albeit slightly less) by increasing salt concentration (7.2 kcal mol^{-1}), whereas for **G2** binding DNA, $T\Delta S_{bind}$ is basically unaffected by salt. We will consider a structural rationale for these differences in more detail later on.

The salt-induced difference in ΔG_{bind} for the (**3×G1**) system (2.5 kcal mol^{-1}) is smaller than the corresponding value obtained for the **G1** system multiplied by a factor of 3 ($1.3 \times 3 = 3.9$ kcal mol^{-1}). This is as expected, because the presence of one ligand bound to the DNA will affect the binding of the second and third ligands. Moreover, in comparing the ΔG_{bind} values reported in Table 4, the affinity ΔG_{bind} for the **3×G1** system is more favorable than that for **G1** multiplied times 3. This is the case under both low and biologically relevant salt concentrations and is in agreement with the cooperative binding observed regarding the condensation of DNA with multiple ligands previously reported.[39] Comparing the binding of three **G1** dendrons to the DNA double helix with one single **G2** molecule, both systems have the same amount of charge involved in the electrostatic interactions (total charge = +27 in both cases). For **G2** and **3×G1** (in both salt concentrations) the enthalpic values for DNA binding are quite similar. However, the **3×G1** system binding DNA is characterized by a smaller entropic cost ($-T\Delta S$) than **G2**. We propose that **G2** loses more degrees of freedom than the three, smaller **G1** molecules, in order to achieve a DNA binding conformation in which all spermine−DNA interactions are optimized. However, the entropic cost of **3×G1** binding DNA is more salt dependent than the binding of **G2**. Clearly the introduction of multiple dendron molecules into the modeling is nontrivial. Therefore, for the remainder of the study, we concentrated on using 1:1 complexes and focused on the effect of salt on the energetics of DNA binding.

In order to probe the binding in more detail, we considered the 1:1 complexes as an assembly of residues. The dendrons were considered to be composed of three different kinds of residue (Figure 4). CEN (yellow) is the benzyl carbamate protecting group at the focal point of the dendron, REP (blue) is the repetitive unit of the Newkome-type dendron (amide-ether repeat unit, Figure 1), and SPM (red) represents the surface spermine groups. This decomposition allowed us to gain insight into the interaction between each individual residue and the DNA double helix and, hence, fully understand the origins of binding.

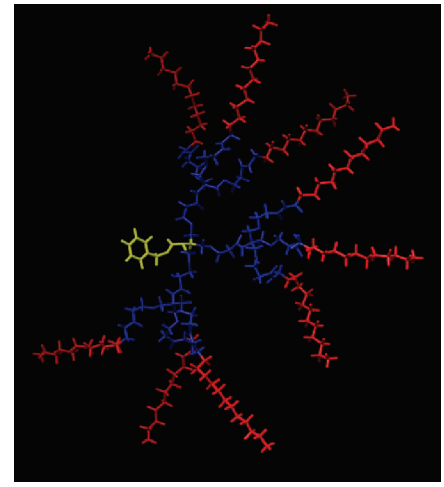

Figure 4. Depiction of **G2** indicating the three different types of structural residue. CEN (yellow), REP (blue), and SPM (red). The SPM ligands are expected to be the primary source of DNA binding affinity.

In Table 5, we consider the energetic values for each residue within the dendron structure. This allows us to look in greater depth at the energetic components of binding. The energetic components reported in Table 5 can be defined in terms of eq 4; that is, they represent the difference between the energy of the dendron/DNA complex ($E_{complex}$) and the sum of the energies of dendron and DNA taken separately ($E_{dendron} + E_{DNA}$). Negative energy values indicate attractive forces and the thermodynamic tendency to form a complex.

$$E_{tot} = E_{complex} - (E_{dendron} + E_{DNA}) \quad (4)$$

Gas-phase energies (E_{gas}) for each residue are composed of electrostatic and van der Waals interaction contributions (E_{ele} and E_{vdw}, respectively) according to eq 5.

$$E_{gas} = E_{ele} + E_{vdw} \quad (5)$$

The *in vacuo* gas-phase energy for each residue (E_{gas}) was then corrected according to solvation to give the total energy E_{tot}. The *mm_pbsa.pl* script of AMBER 9 does not support the Poisson−Boltzmann solvation method for residue energy decomposition, and therefore the generalized Born method was used to correct the gas-phase energies for solvation. Accordingly, the E_{tot} values listed in Table 5 are different from the corresponding ΔH_{bind} values reported in Table 4. However, the

(39) (a) Mel'nikova, Y. S.; Lindman, B. *Langmuir* **2000**, *16*, 5871–5878. (b) Orberg, M.-L.; Schillen, K; Nylander, R. *Biomacromolecules* **2007**, *8*, 157–1563.

Table 5. Interaction Energies Determined for Individual Residues within the **G1** Dendron Structure Interacting with DNA[a]

		9.4 mM NaCl				150 mM NaCl			
residue[f]	number	E_{vdw}[b]	E_{ele}[c]	E_{gas}[d]	E_{tot}[e]	E_{vdw}[b]	E_{ele}[c]	E_{gas}[d]	E_{tot}[e]
CEN	1	−3.3	+11.1	+7.8	−4.1	−5.5	+11.1	+5.6	−5.5
REP	2	−0.6	−11.5	−12.1	−0.1	−0.5	−10.1	−10.6	+0.1
REP	3	−2.3	−25.1	−27.4	−5.4	−2.3	−25.4	−27.7	−5.0
REP	4	−2.8	−11.7	−14.5	−0.9	−2.1	−5.2	−7.3	−0.7
SPM	5	−1.1	−1054.5	−1055.6	−18.0	−0.5	−840.8	−841.3	−11.8
SPM	6	−1.3	−1055.0	−1056.3	−23.4	−2.1	−1145.9	−1147.9	−23.1
SPM	7	−9.7	−1114.5	−1124.2	−22.9	−2.4	−940.3	−942.7	−20.7
total molecule				−3282.3	−74.6			−2971.9	−66.7

[a] Energies represent the difference between the complex and the two individual components. Negative values represent favorable interactions. E_{vdw} and E_{ele} represent van der Waals and electrostatic interaction energies, which are combined to yield the overall *in vacuo* energy, E_{gas}. After correction for solvation, this energy is converted into E_{tot}. All energies are reported in kcal mol^{-1}. [b] E_{vdw} represents the van der Waals interaction energy. [c] E_{ele} represents the electrostatic interaction energy. [d] E_{gas} represents the combination of E_{vdw} and E_{ele} to yield the overall *in vacuo* nonbonded energy. [e] E_{tot} represents the total energy after correction for solvation. [f] CEN represents the central unit at the focal point of the dendron, REP represents the repeat unit of the dendritic architecture, and SPM represents the spermine residues.

Table 6. Differences in Interaction Energies (ΔE) for Each Residue of Dendron **G1** on Changing from Low Salt (9.4 mM) to High Salt Conditions (150 mM)[a]

residue[f]	number	ΔE_{vdw}[b]	ΔE_{ele}[c]	ΔE_{gas}[d]	ΔE_{tot}[e]
CEN	1	−2.2	0.0	−2.2	−1.4
REP	2	0.0	+1.5	+1.5	+0.3
REP	3	0.0	−0.3	−0.3	+0.4
REP	4	+0.7	+6.5	+7.2	+0.2
combined framework				+6.2	−0.6
SPM	5	+0.6	+213.7	+214.4	+6.1
SPM	6	−0.7	−90.9	−91.6	+0.3
SPM	7	+7.3	+174.1	+181.4	+2.2
combined SPM ligands				+302.2	+8.6
total molecule				+308.4	+8.0

[a] Positive data represent a decrease in interaction energy on going from low to high salt conditions. All data are presented in kcal mol^{-1}. [b] E_{vdw} represents the van der Waals interaction energy. [c] E_{ele} represents the electrostatic interaction energy. [d] E_{gas} represents the combination of E_{vdw} and E_{ele} to yield the overall *in vacuo* nonbonded energy. [e] E_{tot} represents the total energy after correction for solvation. [f] CEN represents the central unit at the focal point of the dendron, REP represents the repeat unit of the dendritic architecture, and SPM represents the spermine residues.

trends from the two approaches are in excellent agreement, and this deconvolution approach is particularly useful, as it allows us to determine the relative binding effects of each individual residue. Intuitively, the major contributions to desolvation come from the bound spermine residues, as can be easily derived from the values shown in Table 5 and further in Table 8.

It is clear from Table 5 that the spermine residues are, as expected, primarily responsible for interacting with the DNA double helix. Furthermore, it is evident that this binding can be almost completely ascribed to electrostatic interactions between protonated nitrogens on the spermine ligands and anionic oxygens on the phosphate groups of DNA; that is, E_{ele} dominates the E_{gas} term, while E_{vdw} is negligible. Focusing on spermine residues (SPM) 5, 6, and 7, it is evident that the binding of these units is more uniform at 9.4 mM NaCl than at 150 mM NaCl.

In order to more accurately represent the differences in each of the interaction energies caused by changing the salt concentration, we report in Table 6 the change in each of these parameters (ΔE_{ele}, ΔE_{vdw}, ΔE_{int}, and ΔE_{tot}) as defined by eq 6.

$$\Delta E = E(150\ \text{mM}) - E(9.4\ \text{mM}) \qquad (6)$$

In this analysis, a positive number indicates a large and unfavorable effect of high salt conditions on the interaction energy. In particular, it should be noted that SPM 5 is particularly strongly affected by high salt conditions, with E_{tot} dropping by 6.1 kcal mol^{-1}. It is worth noting that the ΔE_{tot} values derived by this method are in good agreement with the variations in ΔH_{bind} values between 150 and 9.4 mM conditions, which can be derived from Table 4, indicating a pleasing confluence in the way in which these computational approaches deal with the differences caused by changing the salt concentration.

Figure 5 illustrates average snapshots of the dynamic interaction between **G1** and DNA at 9.4 mM (A, C) and 150 mM (B, D) NaCl concentrations. In these images, the SPM residues of **G1** are colored red; everything else in the structure of **G1** is colored yellow. It is evident that at 9.4 mM NaCl all of the SPM groups are involved in the binding and are oriented toward DNA. However, at 150 mM NaCl, the SPM 5 residue is very distant from DNA. This explains why the interaction between SPM 5 and the DNA is significantly weakened under these conditions (Table 6). We reason that the ability of SPM 5 to bind to polyanionic DNA is hindered by the greater quantity of ions in the surrounding solvent, which provide competitive interactions. This observation that there are fewer effective interactions between the SPM ligands of **G1** under high salt conditions and DNA is in agreement with the data in Table 4, which indicated that, for **G1**, the magnitude of ΔH_{bind} decreased by 8.5 kcal mol^{-1} on increasing the NaCl concentration. Furthermore, the structural picture helps explain why $T\Delta S_{bind}$ decreased in magnitude by 7.2 kcal mol^{-1} on increasing the NaCl concentration (Table 4); the binding is less entropically disfavored under high salt conditions as one of the spermine ligands remains unbound to the DNA, hence retaining significant flexibility.

The same analysis was then performed for dendron **G2**. On this occasion, only the data for the SPM residues are reported, as it was determined that they are the crucial residues in the binding process. Table 7 presents the interaction energy data for **G2** with DNA. As in Table 5, the residues reported in Table 7 are numbered in increasing order starting from CEN, through REP to SPM, and since the spermine units are the most crucial in binding, only the values for SPM groups are reported. Table 7 indicates that at high salt levels, SPM units 15, 16, 17, and 18 show the highest magnitude values of E_{gas} and E_{tot}. These units belong to two different sub-branching motifs of **G2**. The third sub-branching motif, which contains SPM 20, 21, and 22, appears to have lower interaction energies when binding to DNA.

Table 7. Interaction Energies Determined for Individual Residues within the **G2** Dendron Structure Interacting with DNA[a]

		9.4 mM NaCl				150 mM NaCl			
residue[f]	number	E_{vdw}[b]	E_{ele}[c]	E_{gas}[d]	E_{tot}[e]	E_{vdw}[b]	E_{ele}[c]	E_{gas}[d]	E_{tot}[e]
SPM	14	−2.8	−921.5	−924.2	−21.4	−2.1	−979.2	−981.3	−18.3
SPM	15	−4.4	−1078.7	−1083.0	−23.9	−3.9	−1141.8	−1145.7	−29.4
SPM	16	−1.8	−1052.2	−1054.0	−19.2	−2.1	−1193.1	−1195.2	−28.9
SPM	17	−8.0	−1177.8	−1185.8	−39.8	−4.9	−1199.0	−1203.9	−36.1
SPM	18	−3.4	−990.1	−993.5	−16.4	−5.1	−1029.7	−1034.9	−23.6
SPM	19	−3.2	−1107.2	−1110.3	−11.1	−0.2	−786.2	−786.4	−9.5
SPM	20	−1.7	−998.9	−999.5	−20.6	−1.0	−953.1	−954.1	−18.1
SPM	21	−1.0	−940.2	−941.1	−19.7	−0.1	−763.3	−763.5	−9.7
SPM	22	−3.8	−959.5	−963.3	−21.7	−3.4	−994.3	−997.7	−18.4
combined SPM ligands				−9254.9	−193.7			−9062.6	−191.9

[a] Energies represent the difference between the complex and the two individual components. Negative values represent favorable interactions. All energies are reported in kcal mol^{-1}. [b] E_{vdw} represents the van der Waals interaction energy. [c] E_{ele} represents the electrostatic interaction energy. [d] E_{gas} represents the combination of E_{vdw} and E_{ele} to yield the overall *in vacuo* nonbonded energy. [e] E_{tot} represents the total energy after correction for solvation. [f] SPM represents the spermine residues.

Table 8. Differences in Interaction Energies (ΔE) for Each Residue of Dendron **G2** on Changing from Low Salt (9.4 mM) to High Salt Conditions (150 mM)[a]

residue[f]	number	ΔE_{vdw}[b]	ΔE_{ele}[c]	ΔE_{gas}[d]	ΔE_{tot}[e]
SPM	14	+0.7	−57.8	−57.1	+3.1
SPM	15	+0.5	−63.2	−62.7	−5.5
SPM	16	−0.3	−140.8	−141.2	−9.7
SPM	17	+3.1	−21.2	−18.1	+3.7
SPM	18	−1.7	−39.6	−41.4	−7.2
SPM	19	+2.9	+321.0	+323.9	+1.6
SPM	20	+0.7	+44.8	+45.4	+2.5
SPM	21	+0.8	+176.8	+177.7	+10.0
SPM	22	+0.5	−34.9	−34.4	+3.3
combined SPM ligands				+192.3	+1.8

[a] Positive data represent a decrease in interaction energy on going from low to high salt conditions. All data are presented in kcal mol^{-1}. [b] E_{vdw} represents the van der Waals interaction energy. [c] E_{ele} represents the electrostatic interaction energy. [d] E_{gas} represents the combination of E_{vdw} and E_{ele} to yield the overall *in vacuo* nonbonded energy. [e] E_{tot} represents the total energy after correction for solvation. [f] SPM represents the spermine residues.

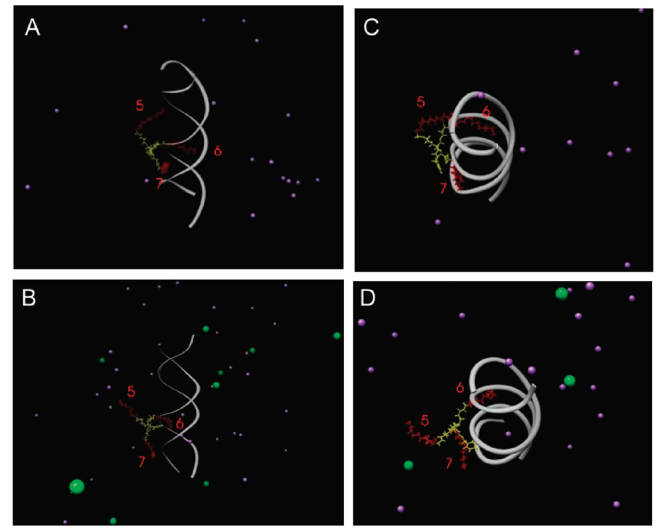

Figure 5. Snapshots of molecular dynamics simulation of dendron **G1** binding to double-helical DNA in the presence of the two different salt concentrations considered. Side views: (A) 9.4 mM NaCl and (B) 150 mM NaCl. Top views: (C) 9.4 mM NaCl and (D) 150 mM NaCl. Within the dendron CEN and REP residues are in yellow and the SPM ligands are shown in red. Water molecules are omitted for clarity, and only the counterions closer to the complexes are shown.

Table 8 quantifies the differences caused by increasing salt concentration. It is evident that some SPM residues are disturbed by NaCl, while the binding of other SPM units to DNA is actually enhanced. For example, it is clear from the E_{gas} values that the interactions of SPM 19, 20, and 21 are adversely affected by the increase in NaCl concentration. However, the binding of the other units to DNA is significantly enhanced on increasing salt concentration, in particular SPM 15, 16, and 18. Overall, this means that the effect of increasing NaCl concentration is minimal on the strength of the complex. Indeed, E_{tot} changes only by 1.8 kcal mol^{-1}, less than 1% of the total. This is in marked contrast with the results for **G1**, where increasing the NaCl decreased the magnitude of E_{tot} by more than 10%. This agrees with the experimental studies, which showed that the binding of **G1** to DNA was adversely affected by NaCl, while the binding of **G2** to DNA was not.

Snapshots of the binding modes are illustrated graphically in Figure 6, allowing us to visualize the data presented in Tables 7 and 8. Importantly, it can be seen that SPM residues 15, 16, 17, and 18 are, under high salt conditions, closest to the DNA double helix and hence forming the most effective interactions. Conversely, SPM 20, 21, and 22 are more distant from the DNA and hence interact with it less effectively. Importantly, focusing on those SPM residues that change their interaction energies on increasing the salt concentration, as the NaCl concentration increases, SPM residues 19, 20, and 21 appear to "sacrifice" their own interaction with the DNA double helix and are turned more toward the external surroundings. Some of these units then form interactions with the chloride ions (e.g., SPM 19); accordingly, ΔE_{tot} is much smaller than the large ΔE_{gas}, as binding to chloride partly compensates for the loss of interaction with DNA. Furthermore, these units act as a kind of barrier, protecting the remaining residues from the surrounding medium, a screening effect. Hence, the interaction between SPM residues 15, 16, and 18 with DNA strengthens, in spite of the higher ionic strength.

This modeling therefore indicates a crucial role that multivalent ligands can play in enhancing binding. The entropic/local concentration benefits of multivalency are well-known and often stated, but in this case, the multivalent ligand plays an active role in enhancing binding under highly competitive conditions. It achieves this by the "sacrifice" of several ligand groups that form interactions with the medium and effectively screen the complex from the electrostatic medium. The remaining ligands are then able to organize their interactions with DNA within this screened region, binding it with enhanced affinity, hence ensuring that binding strength is able to evade the competitive influence. Such medium effects are well-known within dendritic

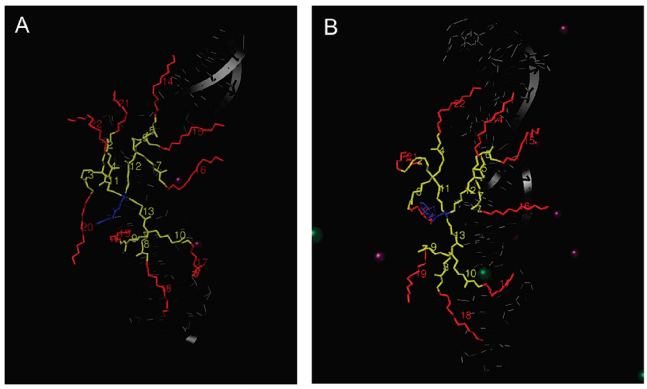

Figure 6. Snapshots of molecular dynamics simulation of dendron **G2** binding to double-helical DNA in the presence of (A) 9.4 mM NaCl and (B) 150 mM NaCl. Within the dendron CEN is shown in blue, REP in yellow, and the SPM ligands in red. The DNA is portrayed as a dark gray shadow, water molecules are omitted for clarity, and only those counterions in close proximity to the complexes are shown.

molecules,[40] but have not previously been suggested to play a role in enhancing multivalent interactions.

We believe that this modeling study therefore suggests a new paradigm in multivalency and demonstrates a new mechanism by which multivalent ligands can exhibit enhanced binding effects in biological systems; that is, although some ligands may not bind to the target under certain conditions, they are nonetheless still playing an active role in enhancing the binding of the remaining ligands. It is important to note that ligand flexibility is vital for this effect to be observed. In the case discussed, the SPM ligands show considerable flexibility, allowing them to effectively move from either (i) binding DNA to acting as a protective barrier (SPM 19, 20, 21) or (ii) binding the DNA with mild affinity to reorganizing so that they can bind it with considerably higher affinity (SPM 15, 16, 18). It is sometimes argued that multivalent ligands may be more effective if they are highly preorganized (and hence rigid). However, this modeling study would indicate that a degree of flexibility in the multivalent display of ligating groups can be highly beneficial in enhancing binding.

Conclusions

In conclusion, we have applied molecular dynamics methods to provide understanding of the interactions between spermine-terminated dendrons **G1/G2** and double-helical DNA. Importantly, we are able to reproduce the binding effects observed experimentally, indicating that this type of modeling is robust and reliable. By considering the dendrons as a series of residues, it becomes possible to deconvolute the energetic effects for the binding of each spermine unit to the DNA double helix. Importantly, it becomes clear that, for **G1**, DNA binding is adversely affected by increasing levels of NaCl (>10% of the binding energy is lost). For **G2** however, we observe a compensation effect, in which some ligands "sacrifice" themselves, losing large amounts of interaction energy with DNA. However, these ligands form a protective barrier for the complex, which screens and optimizes the interaction between other spermine units and the DNA double helix. In this way, the multivalent array is able to maintain high affinity binding as the salt concentration increases, in agreement with, and providing a unique insight into, the experimental results. Clearly, ligand flexibility is of great importance in this case, demonstrating that high levels of preorganization and ligand-framework rigidity are not always beneficial for multivalent recognition processes. This concept of ligand "sacrifice" and binding site screening/optimization proposes a new paradigm in multivalency and indicates a new mechanism by which multivalent ligands may achieve high-affinity binding under a range of conditions.

In the future, we will continue to develop models of dendritic arrays of ligands and attempt to correlate the behavior of the models with that observed experimentally, as well as predicting DNA binding affinities. In particular, issues such as ligand flexibility, dendron structure, and ligand valency are all of key interest. We will also attempt to experimentally verify the new proposals about ligand "sacrifice" and screening/optimization that result from the modeling data presented here. This combination of theoretical and experimental work should allow us to gain unprecedented insight into the multivalent effects that apply in the binding of this class of dendrons to DNA.

Acknowledgment. The generous financial support to the DRUDE Initiative, project "Nanovectors for drug delivery in oncology: a combined modeling/experimental study" performed under the project framework "Computational Life Science promoted by USI" and sponsored by DECS_Canton Ticino to G.M.P., A.D., and S.P., is gratefully acknowledged. D.K.S. also acknowledges EPSRC (C534395/1) in funding this research. All researchers acknowledge the support of COST action TD0802, "Dendrimers in Biomedical Applications", in enabling this collaborative program of research.

JA901174K

(40) See for example: Hawker, C. J.; Wooley, K. L.; Fréchet, J. M. J. *J. Am. Chem. Soc.* **1993**, *115*, 4375–4376. (b) Weyermann, P.; Gisselbrecht, J.-P.; Boudon, C.; Diederich, F.; Gross, M. *Angew. Chem., Int. Ed.* **1999**, *38*, 3215–3219. (c) Smith, D. K. *J. Chem. Soc., Perkin Trans. 2* **1999**, 1563–1565. (d) Koenig, S.; Müller, L.; Smith, D. K. *Chem.—Eur. J.* **2001**, *7*, 979–986. (e) Gorman, C. B. *Adv. Mater.* **1997**, *9*, 1117–1119. (f) Vinogradov, S. A.; Wilson, D. F. *Chem.—Eur. J.* **2000**, *6*, 2456–2461. (g) Collman, J. P.; Fu, L.; Zingg, A.; Diederich, F. *Chem. Commun.* **1997**, 193–194. (h) Stone, D. L.; McGrail, P. T.; Smith, D. K. *J. Am. Chem. Soc.* **2002**, *124*, 856–864.